Supporting Information

Sun et al. 10.1073/pnas.1116821108

SI Materials and Methods

In Vitro Reconstruction of eIF3 Subcomplexes. All eIF3 subunits were PCR amplified from human cDNA (American Type Culture Collection) or were codon-optimized and inserted into transfer vectors 2AT, 2CT, 2GT, 2ST, and 2XT (Table S1, Table S2) using ligation-independent cloning (LIC) (1, 2). The open reading frames for subunits eIF3b (N terminus), eIF3e, eIF3i, and eIF3j were codon-optimized by DNA 2.0 (Table S3). Vectors were developed by the MacroLab at the QB3 Institute, University of California, Berkeley, and are available from Addgene (www.addgene.org).

To prepare the expression vectors for LIC, the 2AT vector was linearized with EcoRV (New England BioLabs) while the 2CT, 2GT, 2ST, and 2XT vectors were linearized with SspI (New England BioLabs). Linearized vectors were gel purified then treated with T4 DNA polymerase (EMD Biosciences) in the presence of dCTP (for 2AT) or in the presence of dGTP (for 2CT, 2GT, 2ST, and 2XT). Oligonucleotides complementary to the target open reading frames were modified with the following 5′ additions:

2AT forward: 5′-TTTAAGAAGGAGATATAGATC-3′

2AT reverse: 5′-TTATGGAGTTGGGATCTTATTA-3′

2(C,G,S, or X)T forward: 5′-TACTTCCAATCCAATGCA-3′

2(C,G,S, or X)T reverse: 5′-TTATCCACTTCCAATGTTATTA-3′

PCR products were purified by gel or using PCR purification columns (Qiagen). PCR products for insertion in vector 2AT were treated with T4 DNA polymerase in the presence of dGTP. Those for insertion into 2(C, G, S, or X)T were treated with DNA polymerase in the presence of dCTP. Plasmids and inserts were combined and transformed into XL1Blue Competent Cells (Agilent). The resulting eIF3-containing transfer vectors are described in Table S1 and Table S2.

Polycistronic expression vectors, also developed by the MacroLab at the QB3 Institute, University of California, Berkeley, and available from Addgene, were constructed by subcloning of the 2(A, C, G, S, or X)T open reading frames into the destination vectors 2D or 2E (Table S1) using five pairs of restriction sites. Briefly, the gene of each eIF3 subunit together with the fusion tag was cut from the 2(A, C, G, S, or X)T transfer vector and ligated into the corresponding cassette of a destination vector. Restriction enzyme pairs for sequential subcloning into the five cassettes of the destination vectors are: 1, XbaI/BamHI; 2, PspXI/AsiSI; 3, SbfI/AscI; 4, NotI/AdeI; and 5, PacI/FseI. The resulting polycistronic vectors containing multiple tagged and untagged eIF3 open reading frames are described in Table S3.

Expression and Purification of eIF3 Subcomplexes. All eIF3 subcomplexes were expressed in Rosetta2(DE3)pLysS *Escherichia coli* (EMD Biosciences), using either ampicillin, kanamycin, or both for selection. Bacterial cultures were grown to an OD at 600 nm of 0.6 at 37 °C, then shifted to 18 °C prior to induction with 0.1 mM IPTG. Cultures were induced for 12 h, harvested by centrifugation, and resuspended in the appropriate lysis buffer, depending on the following chromatography step to be used, as described below. Cells were lysed by sonication on ice and the lysate was clarified by ultracentrifugation at 20,000–30,000 rpm in a Beckman Ti-45 rotor for 20–30 min. The supernatants were filtered with polyethersulfone (PES) membranes with a pore size of 0.45 μm (Nalgene) and loaded on the appropriate HP affinity column (GE Healthcare) to bind the tagged proteins. Individual subunits of eIF3 expressed with N-terminal fusion tags (Table S1, Table S2) were purified by nickel affinity chromatography [His_6-*Saccharomyces cerevisiae* small ubiquitin-like modifier (SUMO) and His_6-γ-crystallin tags], glutathione affinity chromatography (His_6-GST tag), or dextrin sepharose affinity chromatography [His_6-*E. coli* maltose binding protein (MBP) tag].

For nickel affinity chromatography, harvested cells were resuspended in nickel column buffer A (20 mM Hepes, pH = 7.5, 300 mM KCl, 50 mM imidazole, 1 mM DTT, 10% glycerol) containing complete EDTA-free protease inhibitor according to the manufacturer's instructions (Roche Biosciences). The clarified lysate was loaded on a HisTrap HP column (GE Healthcare) and the tagged proteins were eluted on an ÄKTA purifier system by using a linear gradient with nickel column buffer B (20 mM Hepes, pH = 7.5, 300 mM KCl, 500 mM imidazole, 1 mM DTT, 10% glycerol). For the His_6-GST-tagged proteins, harvested cells were resuspended in GST buffer A (20 mM Hepes, pH = 7.5, 300 mM KCl, 1 mM DTT, 10% glycerol) containing complete EDTA-free protease inhibitor according to the manufacturer's instructions (Roche Biosciences). The clarified lysate was loaded on a GSTrap HP column (GE Healthcare) and the GST-tagged proteins were eluted on an ÄKTA purifier system by using a linear gradient with GST buffer B (20 mM Hepes, pH = 7.5, 300 mM KCl, 10 mM reduced glutathione, 1 mM DTT, 10% glycerol). For the His_6-MBP-tagged proteins, cells were resuspended with MBP column buffer A (20 mM Hepes, pH = 7.5, 300 mM KCl, 1 mM EDTA, 1 mM DTT, 10% glycerol) containing complete EDTA-free protease inhibitor according to the manufacturer's instructions (Roche Biosciences). The clarified lysate was loaded on an MBPTrap HP column (GE Healthcare) and the MBP-tagged proteins were eluted on ÄKTA purifier system by using a linear gradient with MBP buffer B (20 mM Hepes, pH = 7.5, 300 mM KCl, 10 mM maltose, 1 mM EDTA, 1 mM DTT, 10% glycerol).

N-terminal tags were cleaved by tobacco etch protease (TEV) in TEV cleavage buffer (20 mM Hepes, pH = 7.5, 300 mM KCl, 1 mM DTT, 10% glycerol) overnight at 4 °C. The cleaved tag and TEV protease were removed from the subunits and complexes by passing the solution through the HisTrap HP column. The flow-through fractions were dialyzed into Q column buffer A (20 mM Hepes, pH = 7.5, 120 mM KCl, 1 mM EDTA, 1 mM DTT, 10% glycerol) for 2 h at 4 °C and passed through a HiTrap Q column (GE Healthcare) with a linear gradient to Q column buffer B (20 mM Hepes, pH = 7.5, 1,000 mM KCl, 1 mM DTT, 1 mM EDTA, 10% glycerol) to remove nonspecifically bound RNA.

Purification of eIF3 Heterodimer Subcomplexes a*c*, gi, and fh. The truncated His_6-SUMO-c*a* dimer (Table S3) was purified by nickel affinity chromatography as described for individual subunits. The N-terminal His_6-SUMO tag was cleaved by TEV Protease in TEV cleavage buffer overnight at 4 °C. The cleaved tag and TEV protease were removed from the dimeric complex by passing the solution through the HisTrap HP column. The flow-through fractions were dialyzed into Q column buffer A for 2 h at 4 °C and passed through a HiTrap Q column (GE Healthcare) with a linear gradient to Q column buffer B to remove nonspecifically bound RNA. Fractions containing the a*c* dimer were pooled together, and further purified by gel filtration over a Superdex 16/60 200 column (GE Healthcare) with the Q column buffer A as running buffer. After gel filtration, purified a*c* dimer, as well as purified c* as an individual subunit were used in binding assays. Purification of tagged gi dimer, starting with coexpression of His_6-SUMO-i and His_6-γ-crystallin-g, and subsequent cleavage by TEV protease to remove the tags, followed

a similar procedure as that for the a*c* dimer. Purification of the fh dimer also followed a similar procedure as that for the a*c* dimer.

Purification of Reconstituted eIF3 Trimers. The trimers His_6-SUMO-c*/a*/ His_6-GST-e, His-SUMO-c*/a*/His_6-GST-l, and His_6-SUMO-c*/a*/His_6-GST-k were coexpressed in *E. coli* as described for individual eIF3 subunits, and purified by glutathione column chromatography, as described above. Similarly, the trimers His_6-SUMO-c*/a*/His_6-MBP-f, His_6-SUMO-c*/a*/His_6-MBP-h, and His_6-SUMO-c*/a*/His_6-MBP-m were purified by dextrin sepharose column chromatography, as described above. All of these trimers were cleaved by TEV protease overnight at 4 °C and purified from the cleaved tags and nonspecifically bound RNA, as described above for the a*c* dimer.

Purification of Reconstituted a*bc*gi, bgi, and a*bc* Subcomplexes. The a*bc*gi, bgi, and a*bc* subcomplexes were expressed in *E. coli* as described for individual eIF3 subunits. Lysates cleared and filtered as described above were loaded onto a 5-mL HisTrap HP column (GE Healthcare). Proteins were fractionated on an ÄKTA FPLC using a linear gradient with nickel column buffer C (20 mM Hepes, pH = 7.5, 300 mM KCl, 400 mM imidazole, 1 mM DTT, 10% glycerol) over 25 column volumes (CV). Fractions were analyzed by SDS-PAGE gel electrophoresis and the correct fractions were pooled together. The pooled fractions were dialyzed in a 10,000 molecular weight cutoff (MWCO) dialysis membrane (Thermo Scientific) in the presence of TEV protease overnight at 4 °C in TEV cleavage buffer. The samples were then passed through the nickel affinity column to remove TEV protease, cleaved tags, and any uncleaved protein.

The flow-through fractions were collected and dialyzed in a 10,000 MWCO dialysis membrane (Thermo Scientific) in buffer AQS (20 mM Hepes, pH = 7.5, 120 mM KCl, 1 mM DTT, 1 mM EDTA, 1 mM EGTA, 10% glycerol) for two hours to reduce the salt concentration from 300 mM KCl to approximately 120 mM KCl. Then, the sample was loaded onto a HiTrap Q column (GE Healthcare) and the protein was eluted using ÄKTA FPLC purification system with a linear gradient to buffer BQS (20 mM Hepes, pH = 7.5, 800 mM KCl, 1 mM DTT, 1 mM EDTA, 1 mM EGTA, 10% glycerol) using a gradient from 0–90% over 25 CV. Fractions were analyzed with SDS-PAGE gels and those with pure complexes were pooled together, concentrated by ultrafiltration, and either frozen in liquid nitrogen and stored at −80 °C or were immediately assayed for binding activity.

Purification of the a*c*efhl Hexameric Subcomplex. For the hexamer a*c*efhl, we cotransformed plasmids 2E containing His_6-SUMO-c*/a*/His_6-MBP-h/His_6-GST-f and 2D containing His_6-GST-e/His_6-GST-l into *E. coli* BL21(DE3) Rosetta cells, and induced expression as described for individual eIF3 subunits. The tagged hexamer was first purified by glutathione affinity chromatography, as described above. The purified and tagged hexamer was then cleaved by TEV protease overnight at 4 °C, as described above. The resulting untagged hexamer was removed from TEV protease, tags, and uncleaved proteins by passing the cleavage reaction over a HisTrap HP column, and collecting the flow-through fractions. The sample was subsequently dialyzed into buffer AQS for purification by anion exchange chromatography. The sample was purified over a 5-mL HiTrap Q column (GE Healthcare), using a 0–100% gradient with buffer BQS, over 20 CV. Pooled fractions from the anion exchange chromatography were then purified by gel filtration chromatography using a Sephacryl S400 column (GE Healthcare) and buffer AQS. The final purified hexamer was either flash-frozen and stored at −80 °C, or used immediately for biochemical assays.

Purification of the a*c*efhlk and a*c*efhlm Heptameric Subcomplexes. For the heptamer a*c*efhlk, we cotransformed plasmids 2E containing His_6-SUMO-c*/a*/His_6-MBP-h/His_6-GST-f and 2D containing His_6-GST-e/His_6-GST-l/His_6-GST-k into *E. coli* BL21(DE3) Rosetta cells; for the heptamer a*c*efhlm, we cotransformed plasmids 2E containing His_6-SUMO-c*/a*/His_6-MBP-h/His_6-GST-f and 2D containing His_6-GST-e/His_6-GST-l/His_6-MBP-m into *E. coli* BL21(DE3) Rosetta cells. The expression and purification of heptamers was carried out as for the a*c*efhl hexamer, as described above.

Purification of the Proteasome, COP9, eIF3 (PCI)/Mpr1-Pad1 N-terminal (MPN) Octamer (a*c*fhelmk). The plasmids used for expression were plasmid 2E containing His_6-SUMO-c*/a*/His_6-MBP-h/His_6-GST-f and plasmid 2D containing His_6-GST-e/His_6-GST-l/His_6-MBP-m/His_6-GST-k. The untagged PCI/MPN octamer was purified as described for the a*c*efhkl hexamer. The final purified PCI/MPN octamer was either flash-frozen and stored at −80 °C, or used immediately for biochemical assays.

Purification of 9-mer through 12-mer eIF3 Subcomplexes. The individual eIF3 subunits His_6-GST-b, His_6-GST-d, His_6-GST-j, and the purified gi dimer described above were used for higher-order assemblies, by addition to the purified PCI/MPN octamer. The tagged subunits were purified as described for individual subunits above, but with the tags retained as needed. The His_6-GST, His_6-SUMO, and His_6-γ-crystallin tags were removed by TEV protease cleavage, and the proteins further purified by anion exchange chromatography (HiTrap Q, GE Healthcare), as described above when needed.

To purify the nonamer a*c*dfhelmk (PCI/MPN octamer plus d), excess purified His_6-GST-d was incubated with untagged PCI/MPN octamer in TEV cleavage buffer overnight at 4 °C, followed by glutathione affinity purification, as described for individual subunits above. The resulting complexes were cleaved with TEV protease and purified as described for the a*c*efhl hexamer. An untagged decameric complex composed of the PCI/MPN octamer plus eIF3 subunits b and d was purified as follows. The nonamer formed above containing uncleaved His_6-GST-d (PCI/MPN octamer plus His_6-GST-d) was incubated with excess purified and untagged eIF3b overnight at 4 °C. Subsequently, the complex was purified by glutathione affinity chromatography and the remaining tag removed, as described for the a*c*efhl hexamer. The dodecameric eIF3 lacking only subunit eIF3j was assembled starting from the purified and tagged decameric complex (PCI/MPN octamer plus b and His_6-GST-d). Excess purified and untagged gi dimer (described above) was incubated with the tagged decamer overnight at 4 °C. Subsequently, the dodecameric complex was purified by glutathione affinity chromatography and the remaining tag removed, as described for the a*c*efhl hexamer.

Purification of eIF3, 40S Ribosomal Subunits and Hepatitis C Viral (HCV) Internal Ribosome Entry Site (IRES) RNAs. Human eIF3 and 40S ribosomal subunits, subunit eIF3j, and the HCV IRES and IIIabc domains were purified as described in refs. 3–6. The sequence of the IRES IIIabc domain is that used in ref. 4. The IRES used in rabbit reticulocyte lysate (RRL) initiation complex formation includes nucleotides 39–352 of the hepatitis C virus subtype 1b genomic RNA.

Labeling of IIIabc Domain of the HCV IRES and Subunit eIF3j. The IIIabc domain of the HCV IRES was labeled at the 3′ end for use in native gel mobility shift assays. The 3′ end of the RNA was first oxidized using 0.1 M sodium periodate in 0.1 M sodium acetate at pH 5 (7). The mixture was incubated in the dark for 90 min at 25 °C and the reaction was stopped by adding 0.25 M KCl and incubating on ice for 10 min. Precipitate was removed by centrifugation at 8,000 × *g* and the supernatant was then passed

through a Sephadex G-25 column (GE Healthcare) to remove salt. The oxidized RNA was then covalently coupled to a hydrazine derivative of fluorescein (Invitrogen Molecular Probes) in a buffer of 0.1 M NaOAc at pH 5 for 4 h at 25 °C. Excess fluorophore was removed by phenol extraction and the RNA was stored frozen at −20 °C. Before use, the IIIabc RNA was refolded at 65 °C for 5 min in THEMK buffer (34 mM Tris, 66 mM Hepes, 0.1 mM EDTA, 2.5 mM $MgCl_2$, 75 mM KCl, pH = 7.8) and kept at room temperature before incubation with eIF3 subcomplexes.

Subunit eIF3j was labeled with Alexa Fluor 488 dye (Invitrogen Molecular Probes). In a labeling reaction, 250 μL of 1.7 mg/mL eIF3j was reduced with 0.25 μL of 1 M DTT and applied to a Nap-25 column (GE Healthcare) preequilibrated with modification buffer (50 mM Hepes, pH = 7.3, 200 mM NaCl, 10% glycerol) to remove DTT. Buffer was also bubbled with N_2 to remove oxygen and prevent oxidation of reduced cysteines. Once eluted from column, eIF3j in 1.5 mL was treated with three molar equivalents of Alexa Fluor 488 dissolved in DMSO to conjugate the fluorophore to cysteines in eIF3j. The reaction was allowed to occur for 2 h at 25 °C, followed by overnight incubation at 4 °C. Excess fluorophore was removed using a Microcon concentrator (MWCO of 10,000, Millipore) the next day.

Purification of Tagged eIF1, eIF1A, and the Central Domain of eIF4G. Tagged versions of eIF1 and eIF1A (His_6-MBP-eIF1A and His_6-MBP-eIF1) were expressed as described above for individual eIF3 subunits. The tagged factors were purified essentially as described in ref. 5. A truncated version of human eIF4G (amino acids 1011–1104) with an N-terminal His_6-FLAG tag (His_6-FLAG-eIF4Gt) was purified using nickel affinity chromatography. The resulting partially purified His_6-FLAG-eIF4Gt was dialyzed in buffer 4gA (20 mM Hepes, pH = 7.5, 50 mM KCl, 1 mM DTT, 10% glycerol) for 2 h. The protein was then loaded on a HiTrap SP column (GE Healthcare), and purified by using a linear 0-90% gradient with buffer BQS over 25 CV. Fractions with purified His_6-FLAG-eIF4Gt were pooled together, concentrated by ultrafiltration, and used in pull-down assays.

EM Sample Preparation. Samples were diluted to a final concentration of 50 nM in imaging buffer (20 mM Hepes, 120 mM KCl, 0.5 mM EDTA, 1 mM DTT, pH = 7.4) supplemented with 3% trehalose. Continuous carbon grids on nitrocellulose were plasma cleaned in a 75% Ar/25% O_2 atmosphere for 20 s in a Solarus plasma cleaner (Gatan, Inc.). To avoid preferential orientation of the specimen, some of the grids were also incubated with a 0.1% (wt/vol) polylysine solution (Polysciences, Inc.) prior to sample deposition (8). Sample aliquots of approximately 4 μL were placed onto the grids, negatively stained with a 3% uranyl acetate solution and blotted dry. Data were acquired using a Tecnai T12 electron microscope operating at 120 keV at a nominal magnification of 50,000X (2.18 Å/pixel). Images were collected using low dose techniques (exposures of ∼20 $e-/Å^2$) within a random focus range from −0.5 to −1.5 μm. Images were automatically recorded using the Leginon data collection software (9) on a Tietz 4 × 4 K pixel CCD camera (15 μm pixel size).

EM Data Processing and Three-Dimensional Reconstruction. All the processing of two-dimensional data was performed using programs and utilities contained within the Appion processing environment (10). Particles were initially extracted using a difference of Gaussians particle picker (11). After contrast transfer function (CTF) estimation using CTFFind (12), particle image stacks were generated by extracting selected particles with a box size of 192 × 192 using the batchboxer program (13) for those images with an estimated CTF confidence cutoff above 80%. The stack was binned by two and reference-free two-dimensional classification was performed using IMAGIC (14) iterative multivariate statistical analysis and multireference alignment analysis (MSA-MRA). The resulting class averages were analyzed by eye and those corresponding to aggregates, overlapping particles or dust were removed prior to subsequent rounds of MSA-MRA. This process was repeated several times until all false or damaged particles were removed. The stacks containing the particles included in the final set of class averages (21,472 and 12,452 particles for the PCI/MPN octamer and dodecamer stacks, respectively) were generated from phase-flipped micrographs using the estimated parameters from the CTFFind program (12).

Three-Dimensional Reconstruction and Difference Map Calculation. The previously determined structure of human eIF3 (15) was filtered at 120-Å resolution and used as initial model. Three-dimensional refinement was performed using iterative projection matching in EMAN2 (13, 16) with initial and final angular steps of 25 and 10 degrees over the course of six iterations. Inner iterations within each of them were repeated until more than 95% of the particles exhibited a pixel error below 1 pixel. The dataset was split into even/odd halves and the Fourier shell correlation (FSC) between the two resulting volumes was used to estimate the resolution using the 0.5 criterion. The resulting volumes were scaled using proc3d within the EMAN package (13) and normalized with Spider (17). The PCI/MPN octamer (filtered to 29 Å) and 12-mer were substracted from one another in chimera to generate difference maps (18).

The 40S Ribosomal Subunit-eIF3 (Sub)complex Formation. Binding reactions were carried out at 25 °C for 15 min in ribosome binding buffer (20 mM Hepes, pH = 7.5, 100 mM KCl, 2.5 mM $MgCl_2$). Native agarose gel electrophoresis used to monitor binding was carried out at 4 °C in THEMK buffer with frequent buffer exchanges.

eIF3 (Sub)complex Interactions with Labeled IIIabc HCV IRES and eif3j-Alexa488. Binding reactions to the IIIabc HCV IRES domain contained reconstituted human eIF3, fluorescently labeled HCV IRES IIIabc domain at 20 nM, and THEMK buffer. The reactions were carried out at 25 °C for 15 min, then resolved by native 1% agarose gels containing THEMK buffer, at 4 °C for 45 min. Similarly, binding of eIF3 subcomplexes to fluorescently labeled eIF3j was assayed by native agarose gels containing THEMK buffer. The resulting agarose gels were analyzed by fluorescence imaging using a Typhoon Scanner (Amersham Biosciences) to detect the gel shifts. The excitation and emission wavelengths to detect the HCV IRES IIIabc domain and eIF3j were 494 and 518 nm, respectively.

eIF1, eIF1A, and eIF4G Pull-Down Assays. For eIF1A or eIF1 pull-down assays, 50 μL of amylose resin (New England BioLabs) was washed three times with MBP column buffer A and then incubated with 20 μg of purified His_6-MBP-eIF1A or His_6-MBP-eIF1 for 1 h at 4 °C with gentle rotation. The beads were pelleted, to allow for removal of the supernatant. Following three washes with MBP column buffer A, 100 μg of purified PCI/MPN octamer was incubated with the beads for 2 h at 4 °C. After removing the supernatant and washing the beads three times, bound proteins were eluted using MBP column buffer B.

A truncated version of human eIF4G (amino acids 1011–1104) with an N-terminal His_6-FLAG tag (His_6-FLAG-eIF4Gt) was used for eIF4G pull-down assays. Pull-down assays were carried out using resin linked to anti-FLAG antibodies (ANTIFLAG M2 affinity gel, Sigma). Briefly, 60 μL of resin slurry were washed three times with 500 μL of dilution buffer (20 mM Hepes pH = 7.5, 150 mM KCl, 10% glycerol), followed by addition of 10 μg of His_6-FLAG-eIF4Gt to allow the FLAG-tagged truncated eIF4G to bind to the resin. The resin was then washed three times with 100 μL wash buffer (20 mM Hepes pH = 7.5, 200 mM KCl, 0.5% Triton X-100, 0.5 mM DTT, 5% glycerol). Natively

purified eIF3 or reconstituted eIF3 complexes were then added to the resin and incubated with the resin for 30 min on ice. The resin was then washed three times with wash buffer to remove unbound protein. Any bound eIF3/eIF4G complex was then eluted by adding 7.5 μg FLAG peptide in dilution buffer.

In Vitro Translation Assays with Reconstituted eIF3. In vitro translation assays were carried out using nuclease-treated RRL (Promega) (19–21). The purification of the 9-subunit and 12-subunit eIF3 complexes containing GST-tagged eIF3d was as described above, but with the GST tag retained prior to the final gel filtration step. Each 200 μL reaction contained 133 μL RRL, supplemented with 1.8 mM $MgCl_2$, 45 mM KCl, 26 mM KOAc, 1.7 mM DTT, 20 μM amino acids, 1.3 U/μL RNasin Plus RNase Inhibitor final concentration (Promega), and Complete Protease Inhibitor Cocktail at the recommended concentration (Roche) (19, 20). After preincubation of approximately 500 nM reconstituted human eIF3 with translation mix on ice for 15 min, translation reactions were initiated by the addition of 1 μM of fluorescently labeled IRES mRNA, followed by incubation at 30 °C for 12 min. To trap initiation complexes, 2 mM GMPPNP was included in the translation reaction. In the case of the non-IRES control, samples were prepared as above, but without inclusion of the IRES RNA. Reaction mixtures were then loaded directly onto 5–20% sucrose gradients in 50 mM Hepes, pH 7.5, 100 mM KOAc, 100 mM NH_4Cl, 10 mM $MgCl_2$, 2 mM DTT, and 0.1 mM EDTA and were centrifuged in a Beckman SW41 rotor at 40,000 rpm for 3.5 h at 4 °C (21). Gradients of the RRL reactions were fractionated using an ISCO UV detector and 0.33 mL fractions were collected for subsequent native agarose gel and affinity purification experiments.

To track the HCV IRES, 10 μL of each fraction was resolved by native agarose gel electrophoresis in THEMK buffer, as described above. Fractions from the sucrose gradients were pooled into four larger fractions (F1-F4), to which additional RNasin Plus RNase Inhibitor and Complete Protease Inhibitor Cocktail were added. The four fractions were then dialyzed into THEMK buffer for 2 h at 4 °C. To affinity purify complexes containing GST-tagged eIF3, the pooled fractions were mixed gently with 0.1 mL reduced Glutathione-Sepharose 4B beads (GE Healthcare) for 2 h at 4 °C. The beads were collected by brief centrifugation and washed three times with THEMK buffer. Complexes bound to the beads were eluted with THEMK buffer containing 10 mM reduced glutathione.

The affinity-purified complexes were then analyzed by Western and Northern blotting, as follows. The presence of GST-eIF3d was probed with an anti-GST antibody (Abcam), as described in ref. 22. Similarly, the presence of eIF2 was probed with an anti-eIF2α antibody (Cell Signaling), and subunit eIF3a or its truncated version (a*) was probed using an anti-eIF3a antibody (Santa Cruz). To probe for the 40S ribosomal subunit and $tRNA_i$, an 18S rRNA-specific probe (5′-ACGGTATCTGATCGTCTTCGAACC-3′) (23) and a $tRNA_i$-specific probe (5′-TGGTAGCAGAGGATGGTTTCGAT-3′) were used. The probes were labeled on the 5′ end with [γ-^{32}P] ATP (Perkin Elmer) using T4 polynucleotide kinase (New England BioLabs).For 18S rRNA Northern blotting analysis, total RNA from the affinity-purified samples was resolved on a 1% agarose gel run with 1x TAE buffer (40 mM Tris, 20 mM acetic acid, and 1 mM EDTA). RNA from the resulting gel was transferred to a nylon membrane using capillary action in 10x SSC buffer (1x SSC buffer contains 150 mM NaCl, 15 mM trisodium citrate, pH 7.0). For $tRNA_i$ Northern blotting analysis, total RNA from the affinity-purified samples was resolved using a 10% polyacrylamide gel in 0.5x TBE buffer (1x TBE buffer contains 89 mM Tris, 89 mM boric acid, and 2 mM EDTA). RNA from the polyacrylamide gel was electroblotted onto a nylon membrane at 20 V for 90 min at 4 °C with 0.5x TBE buffer. The membranes for 18S rRNA and $tRNA_i$ analysis were hybridized with the ^{32}P-labeled probe in ExpressHYb Hybridization Solution (Clontech) at 42 °C overnight. After hybridization, 18S rRNA blots were washed with 2x SSC buffer containing 0.1% SDS at 42 °C for 30 min and then 0.2x SSC containing 0.1% SDS at 42 °C for 30 min. Blots for $tRNA_i$ were washed twice by 20 mL 6x SSC for 5 min at 42 °C and twice by 20 mL 2x SSC and twice by 20 mL 1x SSC. Band intensities on the Northern blotting membranes were quantified by STORM phosphorimager analysis (Molecular Dynamics).

Optimized Open Reading Frames for eIF3 Subunits. The N-terminal nucleotides of eIF3b (nucleotides 1–303) were optimized as follows:

ATGCAAGACGCCGAGAACGTAGCAGTCCCGGAAGCAGCAGAAGAGCGTGCGGAACCGGGCCAGCAGCAACCGGCAGCTGAGCCTCCGCCTGCCGAAGGTCTGCTGCGTCCGGCAGGTCCGGGTGCGCCGGAGGCCGCTGGCACGGAGGCGTCTAGCGAAGAGGTTGGCATCGCGGAAGCCGGTCCGGAAAGCGAGGTGCGCACCGAGCCGGCAGCGGAAGCTGAGGCGGCGAGCGGTCCGAGCGAGAGCCCGTCCCCGCCAGCGGCGGAAGAGTTGCCGGGCAGCCACGCGGAGCCACCGGTT

The coding sequence for human eIF3e was optimized as follows:

ATGGCAGAATACGACTTGACCACCCGCATCGCACATTTTCTGGATCGTCACCTGGTATTCCCGCTGCTGGAGTTCCTGAGCGTGAAAGAGATCTATAATGAGAAAGAACTGTTGCAAGGCAAGCTGGACCTGCTGAGCGATACGAACATGGTGGACTTCGCCATGGATGTCTACAAAAATCTGTATAGCGATGATATTCCGCACGCCCTGCGCGAGAAACGTACTACGGTGGTTGCACAACTGAAGCAATTGCAGGCGGAAACCGAGCCGATTGTTAAGATGTTTGAAGATCCGGAGACTACGCGCCAGATGCAGAGCACGCGCGACGGTCGTATGTTGTTCGACTATCTGGCAGACAAGCACGGTTTTCGTCAGGAGTATCTGGACACCCTGTACCGTTATGCCAAGTTTCAGTATGAGTGTGGCAACTATAGCGGCGCTGCAGAGTACTTGTACTTTTTCCGTGTGCTGGTCCCGGCGACCGACCGTAATGCACTGAGCTCTTTGTGGGGTAAACTGGCGTCGGAGATCCTGATGCAGAATTGGGATGCGGCGATGGAGGACCTGACCCGTCTGAAAGAAACGATTGATAACAACAGCGTATCCAGCCCGCTGCAGAGCCTGCAGCAGCGCACCTGGCTGATTCACTGGTCCCTGTTTGTGTTCTTTAATCATCCGAAGGGCCGTGATAACATTATCGACCTGTTTCTGTACCAGCCGCAGTACTTGAACGCGATTCAGACGATGTGCCCGCATATCCTGCGTTACCTGACCACCGCGGTGATTACCAATAAGGATGTTCGTAAGCGTCGTCAAGTGCTGAAAGACCTGGTGAAAGTCATCCAACAAGAGAGCTACACGTACAAGGACCCAATCACCGAGTTTGTTGAATGCCTGTATGTTAACTTCGACTTCGATGGTGCGCAAAAGAAATTGCGCGAGTGTGAGAGCGTCTTGGTCAACGACTTCTTCCTGGTTGCCTGCTTGGAAGATTTCATTGAGAACGCCCGTCTGTTTATCTTTGAAACGTTTTGTCGTATCCACCAATGCATCTCTATCAACATGCTGGCGGATAAACTGAATATGACCCCGGAAGAAGCCGAGCGTTGGATTGTGAATCTGATTCGCAATGCGCGCCTGGACGCCAAAATTGATAGCAAACTGGGTCACGTCGTTATGGGCAATAACGCGGTTAGCCCTTACCAACAAGTCATCGAGAAAACCAAGAGCCTGTCTTTCCGTAGCCAAATGCTGGCAATGAATATTGAAAAGAAACTGAACCAGAACTCCCGCAGCGAAGCTCCGAATTGGGCGACTCAGGACAGCGGTTTCTATTAA

The coding sequence for human eIF3i was optimized as follows:

ATGAAACCGATCCTGCTGCAAGGCCACGAACGCTCAATCACCCAGATCAAGTACAATCGTGAAGGCGATCTGCTGTTCACGGTCGCCAAGGACCCGATTGTGAACGTTTGGTATAGCGTGAACGGCGAGCGTCTGGGTACCTACATGGGTCACACGGGTGCGGTCTGGTGCGTTGACGCGGACTGGGACACCAAGCACGTCCTGACCGGCAGCGCTGA-

CAACAGCTGCCGCCTGTGGGACTGTGAGACTGGTAAA-
CAGCTGGCCCTGCTGAAAACCAACAGCGCGGTGCGTA-
CGTGTGGTTTCGATTTCGGTGGCAATATCATTATGTTTA-
GCACCGACAAGCAGATGGGTTACCAGTGCTTCGTGAG-
CTTCTTCGACTTGCGCGACCCGTCCCAAATTGACAATA-
ATGAACCGTATATGAAAATTCCGTGCAATGACAGCAA-
GATTACCAGCGCGGTGTGGGGTCCATTGGGTGAGTGT-
ATCATTGCGGGCCATGAGTCTGGTGAGCTGAACCAAT-
ACAGCGCAAAGTCCGGTGAAGTCTTGGTTAACGTTAA-
AGAGCACAGCCGTCAGATCAACGACATTCAACTGAGC-
CGCGATATGACCATGTTTGTGACCGCAAGCAAGGATA-
ACACGGCGAAACTGTTCGATTCCACCACGCTGGAGCA-
CCAAAAGACTTTCCGCACTGAGCGTCCGGTGAACTCT-
GCAGCCCTGTCTCCGAATTATGATCATGTTGTTCTGGG-
CGGTGGTCAAGAGGCTATGGATGTTACGACCACCAGC-
ACGCGTATCGGTAAGTTTGAAGC ACGTTTCTTTCATCT-
GGCGTTTGAAGAAGAATTCGGTCGTGTCAAAGGCC AT-
TTTGGCCCGATCAATTCCGTCGCGTTCCACCCGGATG-
GTAAAAGCTACAGCAGCGGCGGTGAAGATGGCTATGT-
CCGTATTCACTACTTTGATCCTCAGTACTTCGAGTTTGA-
GTTTGAGGCA

The coding sequence for human eIF3j was optimized as follows:

ATGGCCGCTGCAGCAGCGGCTGGCGATAGCGACTC-
CTGGGACGCGGATGCGTTCAGCGTCGAAGATCCGGTT-
CGCAAAGTGGGCGGTGGCGGTACGGCGGGTGGTGAT-
CGTTGGGAGGGTGAGGATGAGGACGAGGACGTCAAA-
GATAACTGGGACGATGACGACGACGAGAAGAAAGAA-
GAGGCCGAGGTCAAACCGGAAGTTAAGATTAGCGAG-
AAGAAGAAAATCGCGGAGAAGATTAAGGAGAAAGAA-
CGTCAACAGAAGAAACGTCAAGAGGAAATCAAAAAG-
CGCCTGGAAGAGCCGGAGGAACCGAAAGTGCTGACC-
CCAGAGGAGCAGCTGGCCGACAAGCTGCGCCTGAAA-
AAGCTGCAGGAAGAATCCGATCTGGAACTGGCGAAA-
GAAACCTTCGGCGTGAATAATGCAGTCTACGGTATCG-
ATGCGATGAATCCGAGCAGCCGTGACGACTTTACCGA-
GTTTGGTAAGCTGTTGAAAGACAAGATCACTCAATAC-
GAGAAGAGCCTGTATTACGCGAGCTTTTTGGAAGTGC-
TGGTTCGTGACGTTTGTATTTCTCTGGAGATTGATGAT-
TTGAAAAAGATCACCAACAGCCTGACGGTGCTGTGCT-
CGGAAAAGCAGAAACAAGAAAAACAGAGCAAAGCAA-
AGAAAAAGAAGAAGGGTGTCGTTCCGGGTGGTGGCC-
TGAAAGCGACCATGAAAGACGATTTGGCCGATTATGG-
TGGCTATGATGGCGGTTACGTTCAAGACTACGAGGAC-
TTCATG

1. Aslanidis C, de Jong PJ (1990) Ligation-independent cloning of PCR products (LIC-PCR). *Nucleic Acids Res* 18:6069–6074.
2. Stols L, et al. (2002) A new vector for high-throughput, ligation-independent cloning encoding a tobacco etch virus protease cleavage site. *Protein Expression Purif* 25:8–15.
3. Damoc E, et al. (2007) Structural characterization of the human eukaryotic initiation factor 3 protein complex by mass spectrometry. *Mol Cell Proteomics* 6:1135–1146.
4. Cai Q, et al. (2010) Distinct regions of human eIF3 are sufficient for binding to the HCV IRES and the 40S ribosomal subunit. *J Mol Biol* 403:185–196.
5. Fraser CS, Berry KE, Hershey JW, Doudna JA (2007) eIF3j is located in the decoding center of the human 40S ribosomal subunit. *Mol Cell* 26:811–819.
6. Kieft JS, Zhou K, Jubin R, Doudna JA (2001) Mechanism of ribosome recruitment by hepatitis C IRES RNA. *RNA* 7:194–206.
7. Dulbecco R, Smith JD (1960) The detection of terminal nucleotide residues in polyribonucleotides. *Biochim Biophys Acta* 39:358–361.
8. Iwanczyk J, et al. (2006) Structure of the Blm10-20 S proteasome complex by cryoelectron microscopy. Insights into the mechanism of activation of mature yeast proteasomes. *J Mol Biol* 363:648–659.
9. Suloway C, et al. (2005) Automated molecular microscopy: The new Leginon system. *J Struct Biol* 151:41–60.
10. Lander GC, et al. (2009) Appion: An integrated, database-driven pipeline to facilitate EM image processing. *J Struct Biol* 166:95–102.
11. Voss NR, Yoshioka CK, Radermacher M, Potter CS, Carragher B (2009) DoG Picker and TiltPicker: Software tools to facilitate particle selection in single particle electron microscopy. *J Struct Biol* 166:205–213.
12. Mindell JA, Grigorieff N (2003) Accurate determination of local defocus and specimen tilt in electron microscopy. *J Struct Biol* 142:334–347.
13. Ludtke SJ, Baldwin PR, Chiu W (1999) EMAN: Semiautomated software for high-resolution single-particle reconstructions. *J Struct Biol* 128:82–97.
14. van Heel M, Harauz G, Orlova EV, Schmidt R, Schatz M (1996) A new generation of the IMAGIC image processing system. *J Struct Biol* 116:17–24.
15. Siridechadilok B, Fraser CS, Hall RJ, Doudna JA, Nogales E (2005) Structural roles for human translation factor eIF3 in initiation of protein synthesis. *Science* 310:1513–1515.
16. Tang G, et al. (2007) EMAN2: An extensible image processing suite for electron microscopy. *J Struct Biol* 157:38–46.
17. Frank J, et al. (1996) SPIDER and WEB: Processing and visualization of images in 3D electron microscopy and related fields. *J Struct Biol* 116:190–199.
18. Goddard TD, Huang CC, Ferrin TE (2007) Visualizing density maps with UCSF Chimera. *J Struct Biol* 157:281–287.
19. Kozak M (1990) Evaluation of the fidelity of initiation of translation in reticulocyte lysates from commercial sources. *Nucleic Acids Res* 18:2828.
20. Berry KE, Waghray S, Doudna JA (2010) The HCV IRES pseudoknot positions the initiation codon on the 40S ribosomal subunit. *RNA* 16:1559–1569.
21. Otto GA, Puglisi JD (2004) The pathway of HCV IRES-mediated translation initiation. *Cell* 119:369–380.
22. Sun C, Pager CT, Luo G, Sarnow P, Cate JHD (2010) Hepatitis C virus core-derived peptides inhibit genotype 1b viral genome replication via interaction with DDX3X. *PLoS One* 5:e12826.
23. Ikeda K, Arao Y, Otsuka H, Kikuchi A, Kayama F (2004) Estrogen and phytoestrogen regulate the mRNA expression of adrenomedullin and adrenomedullin receptor components in the rat uterus. *Mol Cell Endocrinol* 223:27–34.

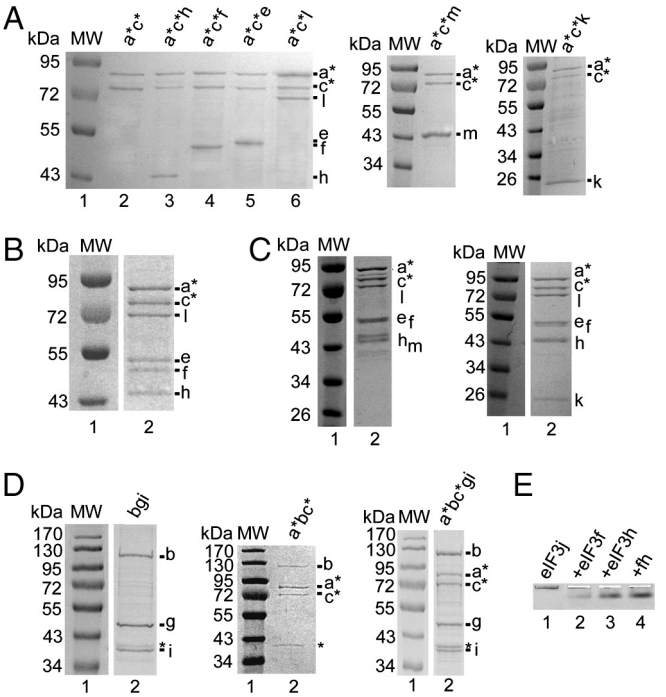

Fig. S1. Reconstitution of eIF3 subassemblies. (*A*) Coomassie blue-stained SDS gels of assembly of trimers involving subunits with PCI or MPN domains. (*B*) Coomassie blue-stained SDS gel of the assembly of an a*c*efhl hexamer, previously identified by limited proteolysis as capable of binding the HCV IRES RNA (*4*), which contains four subunits with PCI domains (a*c*el), and two with MPN domains (fh). (*C*) Assembly of heptamers including subunits with PCI or MPN domains. In all gels, molecular weight markers, in kilodaltons, are shown, and subunit positions are marked to the right. (*D*) Coomassie-blue stained SDS gel of assemblies of oligomers including universally conserved subunits b, g, and i. (*E*) Native agarose gel of eIF3j interactions with subunits eIF3f, eIF3h, and an fh dimer. Subunit eIF3j was used at 10 nM and subunits eIF3f and eIF3h at 30 nM.

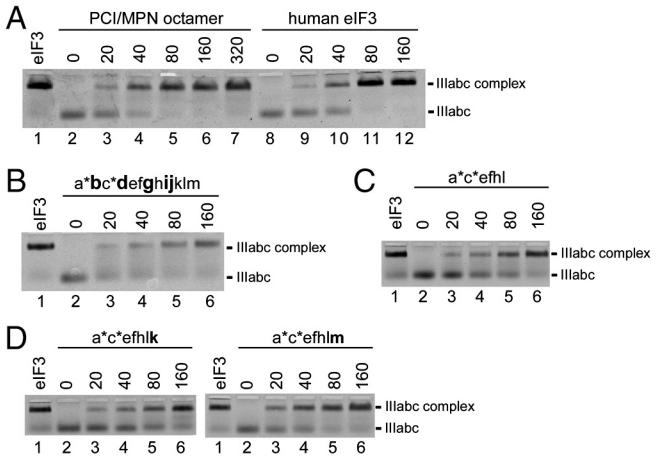

Fig. S2. Binding of eIF3 subassemblies to the HCV IRES IIIabc domain. (*A*) Native agarose gel showing binding of the PCI/MPN octamer or natively purified human eIF3 to the HCV IRES IIIabc domain. The nanomolar concentrations of the octamer and human eIF3 are listed. The PCI/MPN octamer portion of the gel is shown in Fig. 2*A*. (*B*) Native agarose gel showing binding of 13-subunit reconstituted eIF3 binding to the HCV IRES IIIabc domain. The nanomolar concentrations of the 13-mer are listed. The position of the IIIabc RNA/13-mer complex is marked to the right. (*C*) Native agarose gel showing binding of the a*c*efhl hexamer to the HCV IRES IIIabc domain. The nanomolar concentrations of the hexamer are listed. The position of the IIIabc RNA/hexamer complex is marked to the right. (*D*) Native agarose gel of heptamers a*c*efhlk and a*c*efhlm binding to the IIIabc RNA. In all of the experiments, fluorescent IIIabc RNA was used at 20 nM in concentration, and the reactions were carried out in the presence of 2 μM tRNA to prevent nonspecific binding. The experiments in *C* and *D* were carried out immediately after gel filtration of the hexamer and heptamer complexes to remove aggregates.

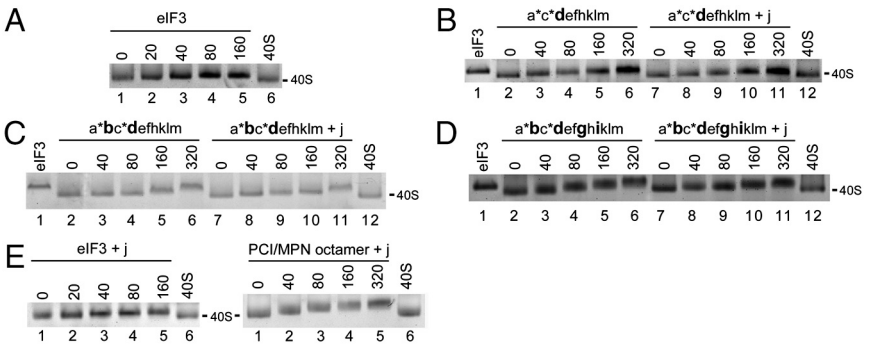

Fig. S3. Binding of eIF3 subassemblies to the 40S ribosomal subunit. (*A*) Native agarose gel showing binding of natively purified human eIF3 to the human 40S ribosomal subunit. The nanomolar concentrations of human eIF3 are listed. (*B*) Native agarose gel showing binding of a nonamer form of reconstituted eIF3 (PCI/MPN octamer plus subunit d, in bold) to the 40S ribosomal subunit, with or without the presence of unlabeled eIF3j. (*C*) Native agarose gel as in *B*, except with the decamer form of reconstituted eIF3 (PCI/MPN octamer purified with eIF3d and eIF3b, in bold). (*D*) As in *B*, except with the dodecamer form of reconstituted eIF3 (PCI/MPN octamer purified with eIF3d, eIF3b, eIF3g, and eIF3i, in bold). (*E*) Native agarose gels as in *A* of natively purified eIF3 or the PCI/MPN octamer binding to the 40S ribosomal subunit in the presence of eIF3j. In all gels, the nanomolar concentrations of eIF3, reconstituted eIF3 assemblies, and eIF3j are given. The 40S ribosomal subunit was used at a concentration of 10 nM.

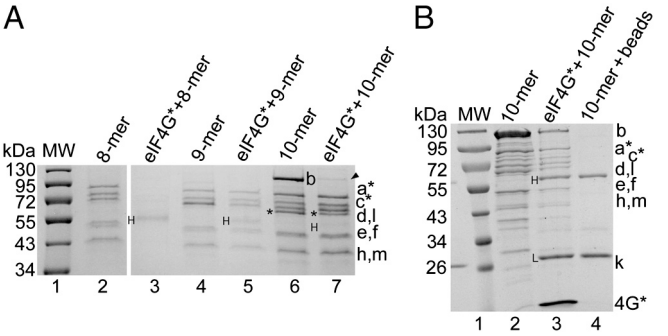

Fig. S4. Binding of eIF3 subassemblies to the central domain of translation factor eIF4G. (*A*) SDS gel showing reconstituted eIF3 10-mer binding to the FLAG-tagged central domain of eIF4G. Samples were affinity-purified by using anti-FLAG antibody beads. Molecular weight (MW) markers are shown to the left. Arrow indicates the position of subunit eIF3b. Asterisks indicate the position of GroE that copurified with eIF3d, as determined by MS analysis. The position of the central domain of eIF4G is below the bottom of the gel region shown. A concentration of 120 mM KCl was used in the washes, less stringent conditions than those used in Fig. 2*D* (compare lanes 4, 5, and 7 in the two gels). (*B*) SDS gel showing specificity of reconstituted eIF3 10-mer binding to the FLAG-tagged central domain of eIF4G, under less stringent conditions compared to Fig. 2*E*. Samples were affinity-purified by using anti-FLAG antibody beads. MW markers are shown to the left. Although some degradation has occurred in this sample, 120 mM KCl in the wash buffer prevented nonspecific binding to the anti-FLAG beads (lane 4). Furthermore, subunit eIF3b remained in the affinity-purified eIF3 complex. The positions of antibody heavy (H) and light (L) chains are marked.

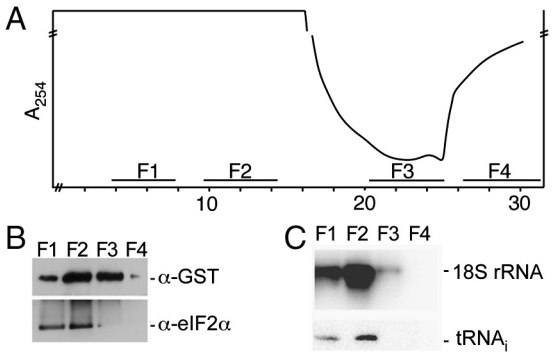

Fig. S5. In vitro 43S preinitiation complex formation in the presence of recombinant eIF3 dodecamer. (*A*) Sucrose gradient of RRL translation reaction stalled with GMPPNP but not programmed with HCV IRES mRNA. The top of the gradient is to the left, and the A_{254} absorbance is shown. The break marked on the absorbance axis corresponds to a decrease of sensitivity to account for heme absorbance. Fractions pooled for GST-affinity purification and analysis are marked and numbered F1-F4. (*B*) Western blotting of GST-eIF3d and eIF2α, from samples GST-affinity-purified from pooled fractions F1-F4 in *A*. (*C*) Northern blotting of 18S rRNA and $tRNA_i$ present in GST-affinity-purified complexes from pooled fractions F1-F4 in *A*.

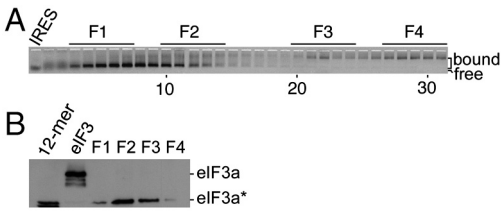

Fig. S6. In vitro translation initiation complex formation in the presence of recombinant eIF3 dodecamer. (*A*) Native agarose gel of individual fractions from the sucrose gradient of the recombinant eIF3 dodecamer experiment in Fig. 3 *A*. The position of fluorescent HCV IRES mRNA is marked, as are the positions of the pooled fractions F1-F4 from the sucrose gradient. (*B*) Western blotting of eIF3a from samples GST-affinity-purified from pooled fractions F1-F4 in Fig. 3*A*. Purified 12-subunit eIF3 and natively purified eIF3 are shown as markers for truncated eIF3a* and for full-length eIF3a, respectively. In this experiment, recombinant eIF3 dodecamer must compete with endogenous eIF3 to form initiation complexes.

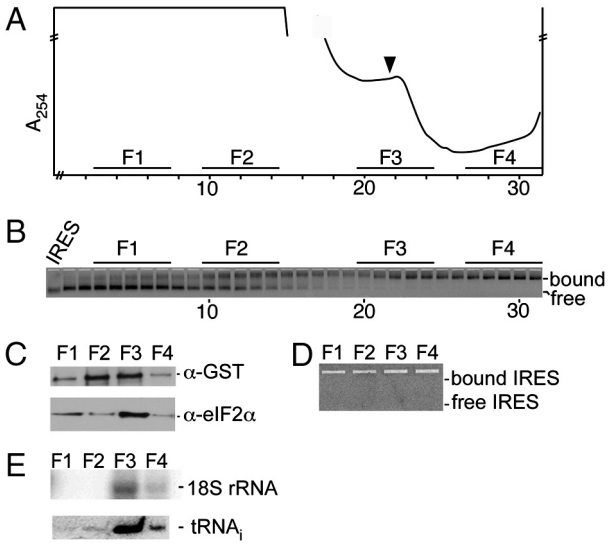

Fig. S7. In vitro translation initiation in the presence of recombinant eIF3 nonamer. (*A*) Sucrose gradient of RRL translation reaction stalled with GMPPNP and programmed with fluorescently labeled HCV IRES-containing mRNA. The top of the gradient is to the left, and the A_{254} absorbance is shown. The break marked on the absorbance axis corresponds to a fivefold decrease of sensitivity to account for heme absorbance. Fractions pooled for GST-affinity purification and analysis are marked and numbered F1-F4, with F3 corresponding to HCV IRES-mediated initiation complexes (arrow). (*B*) Native agarose gel of individual fractions from the sucrose gradient in *A*. The position of fluorescent HCV IRES mRNA is marked, as are the positions of the pooled fractions F1-F4 from the sucrose gradient. (*C*) Western blotting of GST-eIF3d and eIF2α, from samples GST-affinity-purified from pooled fractions F1-F4 in *A*. (*D*) Native agarose gel of fluorescently labeled HCV IRES copurified with GST-tagged eIF3. Samples GST-affinity-purified from pooled fractions F1-F4 in *A* are shown. Note that this gel is contiguous with the native gel shown in Fig. 3*C*, and the two in vitro translation experiments were performed in parallel. (*E*) Northern blotting of 18S rRNA and $tRNA_i$ present in GST-affinity-purified complexes from pooled fractions F1-F4 in *A*. In this experiment, recombinant eIF3 nonamer must compete with endogenous eIF3 to form initiation complexes.

Table S1. N-terminal tag *Escherichia coli* T7 expression vectors used in this study

Vector	Addgene no.	N-terminal tag	Expression host	Resistance, plasmid origin	Type of vector	Tag(s) (kDa)	pI
2AT	29665	yORF	*E. coli T7**	AMP/ColE1	Transfer	NA	NA
2CT	29706	His_6-MBP-N10-TEV-yORF	*E. coli T7*	AMP/ColE1	Transfer	45	5.32
2GT	29707	His_6-GST-TEV-yORF	*E. coli T7*	AMP/ColE1	Transfer	28	6.17
2MT	29708	His_6-MBP-TEV-yORF	*E. coli T7*	AMP/ColE1	Transfer	43	5.32
2ST	29711	His_6-SUMO-TEV-yORF	*E. coli T7*	AMP/ColE1	Transfer	14	5.42
2XT	29714	His_6- gCrystallin-TEV-yORF	*E. coli T7*	AMP/ColE1	Transfer	24	6.55
2D	29774	poycistronic destination vector	*E. coli T7*	AMP/ColE1	Destination	NA	NA
2E	29775	poycistronic destination vector	*E. coli T7*	KAN/ColE1	Destination	NA	NA

yORF, open reading frame; His_6, hexahistidine sequence; MBP, *E. coli* maltose binding protein; TEV, tobacco etch protease cleavage site; GST, *Schistosoma japonicum* glutathione-*S*-transferase; SUMO, *Saccharomyces cerevisiae* small ubiquitin-like modifier; γ-crystallin, human gamma-crystallin; AMP, ampicillin; KAN, kanamycin
**E. coli* expressing T7 RNA polymerase, IPTG inducible.

Table S2. N-terminal tag sequences in *Escherichia coli* T7 expression vectors used in this study

Vector	Amino acid sequence of tags with yORF, ^=TEV, or HRV site
2AT	yORF
2CT	MKSSHHHHHHGSSMKIEEGKLVIWINGDKGYNGLAEVGKKFEKDTGIKVTVEHPDKL EEKFPQVAATGDGPDIIFWAHDRFGGYAQSGLLAEITPDKAFQDKLYPFTWDAVRY NGKLIAYPIAVEALSLIYNKDLLPNPPKTWEEIPALDKELKAKGKSALMFNLQEPYFTW PLIAADGGYAFKYENGKYDIKDVGVDNAGAKAGLTFLVDLIKNKHMNADTDYSIAEA AFNKGETAMTINGPWAWSNIDTSKVNYGVTVLPTFKGQPSKPFVGVLSAGINAAS PNKELAKEFLENYLLTDEGLEAVNKDKPLGAVALKSYEEELAKDPRIAATMENAQKG EIMPNIPQMSAFWYAVRTAVINAASGRQTVDEALKDAQTNSSSNNNNNNNNNNL GIEENLYFQ^SNA(yORF)
2GT	MGSSHHHHHHGSSMSPILGYWKIKGLVQPTRLLLEYLEEKYEEHLYERDEGDKWR NKKFELGLEFPNLPYYIDGDVKLTQSMAIIRYIADKHNMLGGCPKERAEISMLEGAVL DIRYGVSRIAYSKDFETLKVDFLSKLPEMLKMFEDRLCHKTYLNGDHVTHPDFMLY DALDVVLYMDPMCLDAFPKLVCFKKRIEAIPQIDKYLKSSKYIAWPLQGWQATFGGGD HPPKGIEENLYFQ^SNA(yORF)
2MT	MGSSHHHHHHGSSMKIEEGKLVIWINGD KGYNGLAEVGKKFEKDTGIKVTVEHPDKLEEKFPQVAATGDGPDIIFWAHDRFGGYA QSGLLAEITPDKAFQDKLYPFTWDAVRYNGKLIAYPIAVEALSLIYNKDLLPNPPKTW EEIPALDKELKAKGKSALMFNLQEPYFTWPLIAADGGYAFKYENGKYDIKDVGVDNA GAKAGLTFLVDLIKNKHMNADTDYSIAEAAFNKGETAMTINGPWAWSNIDTSKVNY GVTVLPTFKGQPSKPFVGVLSAGINAASPNKELAKEFLENYLLTDEGLEAVNKDKPL GAVALKSYEEELAKDPRIAATMENAQKGEIMPNIPQMSAFWYAVRTAVINAASGRQ TVDEALKDAQTNGIEENLYFQ^SNA(yORF)
2ST	MGSSHHHHHHGSSMASMSDSEVNQEAKPEVKPEVKPETHINLKVSDGSSEIFFKIK KTTPLRRLMEAFAKRQGKEMDSLRFLYDGIRIQADQTPEDLDMEDNDIIEAHREQIG GIEENLYFQ^SNA(yORF)
2XT	MKSSHHHHHHGSSMSKTGTKITFYED KNFQGRRYDCDCDCADFHTYLSRCNSIKVEG GTWAVYERPNFAGYMYILPQGEYPEYQRWMGLNDRLSSCR AVHLPSGGQYKIQIFEKGDFSGQMYETTEDCP SIMEQFHMREIHSCKVLEGVWIFYELPNYRGRQ YLLDKKEYRKPIDWGAASPAVQSFRRIVEGIEENLYFQ^SNA(yORF)

yORF, your open reading frame; TEV, tobacco etch protease cleavage site; HRV, human rhinovirus

Table S3. Constructs in destination vectors

Vector	Construct	Cassette I	Cassette II	Cassette III	Cassette IV	Cassette V
2D	el*	e[†] (2GT)[‡]	—	l (2GT)	—	—
2D	gi	i[†] (2ST)	g (2XT)	—	—	—
2D	bgi	i[†] (2ST)	g (2XT)	b[†] (2AT)	—	—
2D	elm	e[†] (2GT)	—	l (2GT)	m (2CT)	—
2D	elk	e[†] (2GT)	—	l (2GT)	—	k (2GT)
2D	elmk	e[†] (2GT)	—	l (2GT)	m (2CT)	k (2GT)
2D	a*bc*gi	i[†] (2ST)	g (2XT)	c*[§] (2ST)	a*[§] (2AT)	b[†] (2AT)
2E	a*c*	c*[§] (2ST)	a*[§] (2AT)	—	—	—
2E	a*c*f	c*[§] (2ST)	a*[§] (2AT)	f (2CT)	—	—
2E	a*c*h	c*[§] (2ST)	a*[§] (2AT)	h (2CT)	—	—
2E	a*c*e	c*[§] (2ST)	a*[§] (2AT)	e[†] (2GT)[‡]	—	—
2E	a*c*l	c*[§] (2ST)	a*[§] (2AT)	l (2GT)	—	—
2E	a*c*k	c*[§] (2ST)	a*[§] (2AT)	k (2GT)	—	—
2E	a*c*m	c*[§] (2ST)	a*[§] (2AT)	m (2CT)	—	—
2E	a*bc*	b[†] (2AT)	c*[§] (2ST)	a*[§] (2AT)	—	—
2E	a*c*hf	c*[§] (2ST)	a*[§] (2AT)	h (2CT)	—	f (2GT)

*The constructs are designated by eIF3 subunit letter name, all in lower case, i.e., construct el contains human eIF3 subunits eIF3e and eIF3l.

[†]Subunits e, i, and nucleotides 1–303 of subunit b were codon-optimized, as shown *SI Materials and Methods*.

[‡]Transfer vectors in parentheses, with associated tags described in Table S2.

[§]Subunit a* includes amino acids 5–654. Subunit c* includes amino acids 302–913.